

Measurement report: Variations in surface SO₂ and NO_x mixing ratios from 2004 to 2016 at a background site in the North China Plain

Xueli Liu¹, Liang Ran², Weili Lin^{1*}, Xiaobin Xu³, Zhiqiang Ma⁴, Fan Dong⁴, Di He⁴, Liyan Zhou⁴, Qingfeng Shi⁴, and Yao Wang⁴

¹Key Laboratory of Ecology and Environment in Minority Areas (Minzu University of China), National Ethnic Affairs Commission, Beijing 100081, China

²Key Laboratory of Middle Atmosphere and Global Environment Observation, Institute of Atmospheric Physics, Chinese Academy of Sciences, Beijing, 100089, China

³Chinese Academy of Meteorological Sciences, Beijing, 100081, China

⁴Beijing Shangdianzi Regional Atmosphere Watch Station, Beijing, 101507, China

Correspondence to: Weili Lin (linwl@muc.edu.cn)

1 **Abstract.** Strict air pollution control strategies have been implemented in recent decades in the North China Plain
2 (NCP), previously one of the most polluted regions in the world, and have resulted in considerable changes in
3 emissions of air pollutants. However, little is so far known about the long-term trends of the regional background
4 level of NO_x and SO₂, along with the increase and decrease processes of regional emissions. In this study, the
5 seasonal and diurnal variations of NO_x and SO₂ as well as their long-term trends at a regional background station in
6 the NCP were characterized from 2004 to 2016. On average, SO₂ and NO_x mixing ratios were 5.7 ± 8.4 ppb and
7 14.2 ± 12.4 ppb, respectively. The seasonal variations in SO₂ and NO_x mixing ratios showed a similar pattern with a
8 peak in winter and a valley in summer. However, the diurnal variations in SO₂ and NO_x mixing ratios greatly
9 differed for all seasons, indicating different sources for SO₂ and NO_x and meteorological effects on their
10 concentrations. Overall, the annual mean SO₂ exhibited a significant decreasing trend of -6.1% yr⁻¹ ($R = -0.84$, $P <$
11 0.01) from 2004 to 2016, which is very close to -6.3% yr⁻¹ of the annual SO₂ emission in Beijing, and a greater
12 decreasing trend of -7.4% yr⁻¹ ($R = -0.95$, $P < 0.01$) from 2008 to 2016. The annual mean of NO_x showed a
13 fluctuating rise of $+3.4 \%$ yr⁻¹ ($R = 0.38$, $P = 0.40$) from 2005 to 2010, reaching the peak value (16.9 ppb) in 2010,
14 and then exhibited an extremely significant fluctuating downward trend of -4.5% yr⁻¹ ($R = 0.95$, $P < 0.01$) from
15 2010 to 2016. After 2010, the annual mean NO_x mixing ratios correlated significantly ($R = 0.94$, $P < 0.01$) with the
16 annual NO_x emission in North China. The decreasing rate (-4.8% yr⁻¹, $R = -0.92$, $P < 0.01$) of the annual mean
17 NO_x mixing ratios from 2011 to 2016 at the Shangdianzi (SDZ) regional atmospheric background station are lower
18 than the one (-8.8% yr⁻¹, $R = -0.94$, $P < 0.01$) for the annual NO_x emission in the NCP and (-9.0% yr⁻¹, $R = -0.96$,

19 $P < 0.01$) in Beijing. It indicated that surface NO_x mixing ratios at SDZ had weaker influence than SO_2 by the
20 emission reduction in Beijing and its surrounding areas in the NCP. The increase in the amount of motor vehicles
21 led to an increase in traffic emissions for NO_x . This study supported conclusions from previous studies that the
22 measures taken for controlling NO_x and SO_2 in the NCP in the past decades were generally successful. However,
23 NO_x emission control should be strengthened in the future.

24 **1 Introduction**

25 Acid gases sulfur dioxide (SO_2) and nitrogen oxides (NO_x) are closely related to climate, ecology, environment and
26 human health. They are important gaseous pollutants in China (Xu et al., 2009) and also recommended by the
27 Global Atmosphere Watch (GAW) of the World Meteorological Organization (WMO) for priority observation
28 (WMO, 2001). They can also be transformed into nitrate and sulfate aerosols, which play an important role in the
29 formation of aerosol pollution and acid rain (Yang et al., 2011; Cheng et al., 2013; Luo et al., 2016; Chen et al.,
30 2017a). Sulfate and nitrate constitute more than 1/3 of $\text{PM}_{2.5}$ mass concentration and can cause serious respiratory
31 diseases (Yang et al., 2010; Yang et al., 2011; Gao et al., 2012; Zhao et al., 2013; Liu et al., 2014a).

32 With the economic development, population growth and rapid urbanization, air pollution in China exhibited the
33 characteristics of regional pollution centering urban areas in recent years (Shao et al., 2006; Xu et al., 2008). Many
34 studies thereby focused on regional pollution (Qi et al., 2012; Li et al., 2015), instead of local and suburban
35 pollution as previously did (Liu et al., 2008; Lin et al., 2009a). Local/suburban pollution is closely associated air
36 pollutants emitted locally and limited on a smaller scale such as a town, a city or an urban area. Regional pollution
37 occurs over the whole region and is usually associated with large-scale emissions and significantly influenced by
38 transport and accompanying processes, such as chemical reactions, deposition, etc. In China, city clusters have been
39 formed for decades, air pollution often shows regional characteristics. Especially, the North China Plain (NCP)
40 region, a heavily industrialized and densely populated area with considerable agricultural activities, is one of the
41 most polluted regions of the world. The strong emissions of SO_2 and NO_x in the NCP showed the typical regional
42 characteristics (Wu et al., 2010; Lin et al., 2012; Liu et al., 2014b), i.e., similar changes in seasonal and diurnal
43 patterns of NO_x and SO_2 had been observed at different types of sites in this region in previous studies. Previous
44 studies have combined observations at the background site and the urban site for comparisons (Liu et al., 2014b), or
45 selected short-term observations (1–2 years or 1–2 seasons) for the comparative study before and after major
46 activities, in order to quantitatively evaluate the effect of implementing control measures during the event (Cheng et

47 al., 2015; Li et al., 2019; Lin et al., 2011a; Lin et al., 2012; Wei et al., 2016; Wu et al., 2010; Zhong et al., 2020).
48 Most of the long-term studies (more than 10 years) evaluated the temporal and spatial variations of SO₂ and NO_x
49 based on satellite measurements of the vertical column density (Zhang et al., 2007; Cai et al., 2018; Shikwambana et
50 al., 2020). However, there were few studies on the long-term trend of SO₂ and NO_x based on ground-level
51 observations (Bai et al., 2015), especially in the background area of the NCP and with a time span of more than 10
52 years.

53 In this study, we analyzed the long-term variations in surface SO₂ and NO_x mixing ratios observed at a regional
54 WMO GAW station in the NCP, and discussed their influencing factors and their responses to pollution control
55 measures, so as to provide scientific basis for designing further strategies for controlling SO₂ and NO_x on a regional
56 scale.

57 **2 Data and methods**

58 Surface SO₂ and NO_x mixing ratios were measured at the Shangdianzi (SDZ) regional atmospheric background
59 station (117°07' E, 40°39' N, 293.3 m a.s.l.). SDZ is located in Shangdianzi Village in Miyun District of Beijing,
60 China. It is about 110 km northeast of urban Beijing. The measurements of air pollutants at this site could represent
61 the background conditions in the NCP (Lin et al., 2008; Meng et al., 2009a).

62 SDZ is situated on the north hill side of a northeast-to-southwest valley, with farmlands in the south. Corn and
63 wheat were the main crops, but were recently replaced by fruit trees. It lies in a warm temperate and semi-humid
64 climate zone, with short spring and autumn but long winter and summer. The monthly averages of meteorological
65 parameters such as temperature (T), pressure (P), precipitation (PRCP), relative humidity (RH), wind speed (WS)
66 and wind direction are shown in Fig. 1. Precipitation occurs mainly in summer. The prevailing wind directions were
67 from NE–ENE and WSW–SW. Stronger wind speeds appear in spring and weaker in summer.

68 In-situ measurements of SO₂ and NO_x mixing ratios were made using a pulsed fluorescence SO₂ analyzer (Model
69 43C-TL, Thermo Fisher Scientific, MA, USA) and a chemiluminescence NO_x analyzer (Model 42C-TL, Thermo
70 Fisher Scientific, MA, USA), respectively. The detection limits of the Model 43C-TL SO₂ analyzer and the Model
71 42C-TL NO_x analyzer are 0.05 ppb (300 second averaging time) and 0.05 ppb (120 second averaging time),
72 respectively. In Model 42C-TL NO_x analyzer, NO₂ is converted to NO by a molybdenum NO₂-to-NO converter
73 heated to about 325°C. The conversion efficiency was checked annually using gas phase titration of an NO standard
74 with O₃. The converter was replaced if the conversion efficiency was found lower than 96%. The drawback in this

75 NO₂ converter was known to suffer from the interference of other NO_y compounds such as PAN and HNO₃
76 (Steinbacher et al., 2007; Jung et al., 2017), which was also discussed in Yin et al. (2022). As it is not possible in
77 our case to remove the interference, the reported NO₂ and NO_x levels should be treated as upper limits. In order to
78 obtain long-term trends of atmospheric components at a regional atmospheric background station, the observations
79 are required to be accurate, reliable, and comparable. Therefore, strict and effective quality control measures were
80 implemented during the observation (Lin et al., 2019). Daily zero and span checks were routinely and automatically
81 carried out. Multi-point calibrations were done monthly. The standard gases used at the site were compared against
82 NIST-traceable standard gases to ensure the data comparability (Lin et al., 2009b). During the period from January
83 2005 to May 2017, the percentages of effective hourly mean data of SO₂ and NO_x are 97.1 % and 96.7 %,
84 respectively. The wind speed (WS), wind direction (WD), air temperature (T), precipitation (PRCP), relative
85 humidity (RH), and atmospheric pressure (P) during the same period are from the routine meteorological
86 observations. We used a hybrid single-particle Lagrangian integrated trajectory model (Hysplit4.9) from National
87 Oceanic and Atmospheric Administration, USA, with the NCEP–NCAR reanalysis meteorological data set
88 (<https://ready.arl.noaa.gov/archives.php>) to calculate the atmospheric mixed layer heights.

89 **3 Results**

90 **3.1 Observational levels**

91 The time series and statistic results of hourly mean SO₂ and NO_x mixing ratios during the observational period at
92 SDZ are showed in Fig. 2 and Table 1, respectively. The hourly mean SO₂ mixing ratios ranged from 0.01 to 100.34
93 ppb, with 193 hours (0.18 %) exceeded the limit of 57 ppb set in China National Ambient Air Quality Standard
94 (GB3095–2012, Grade I). The hourly mean NO₂ mixing ratios ranged from 0.01 to 124.4 ppb, with 5 hours
95 exceeding the limit of 106 ppb (GB3095–2012, Grade I). The SO₂ mixing ratios exhibited an extremely significant
96 downward trend ($-0.37 \text{ ppb yr}^{-1}$, $R = -0.20$, $P < 0.01$) during the measurement period and a higher downward trend
97 ($-1.10 \text{ ppb yr}^{-1}$, $R = -0.22$, $P < 0.01$) from 2013 to 2017. The NO_x mixing ratios exhibited a much smaller but
98 significant downward trend ($-0.03 \text{ ppb yr}^{-1}$, $R = -0.01$, $P < 0.05$). Details in the trends and the influencing factors
99 will be discussed in Sect. 3.4.

100 As shown in Table 1, the average values $\pm 1\sigma$ (standard deviation) of SO₂, NO, NO₂, and NO_x concentrations are 5.7
101 ± 8.4 ppb, 1.1 ± 2.6 ppb, 13.1 ± 10.9 ppb, and 14.2 ± 12.4 ppb, respectively. The results were close to the annual
102 average concentrations of SO₂ (5.9 ± 10.0 ppb), NO (0.8 ± 2.0 ppb), NO₂ (13.8 ± 13.1 ppb), and NO_x (14.5 ± 14.0

103 ppb) at SDZ in 2004 reported by Meng et al. (2009a). Compared with other background stations in China (Table 2),
104 the SO₂ and NO_x mixing ratios at SDZ are both at a relatively high level.

105 **3.2 Monthly variations**

106 Surface SO₂ and NO_x mixing ratios at SDZ showed a similar seasonal pattern with high values in winter and low
107 values in summer (Fig. 3). The highest SO₂ level appeared in winter (9.5 ppb) with the maximum monthly mean in
108 February (10.6 ppb), followed by that in spring (7.3 ppb) and autumn (5.0 ppb), and the lowest in summer (2.1 ppb)
109 with the minimum in July (1.5 ppb). The concentration of NO_x was higher in winter (18.1 ppb) and autumn (16.5
110 ppb), lower in spring (13.0 ppb) and summer (9.2 ppb). The maximum monthly mean NO_x appeared in November
111 (21.7 ppb) and the minimum one in August (8.7 ppb). The seasonal patterns of SO₂ and NO_x at SDZ were similar to
112 those in urban and rural areas in North China (Meng et al., 2009b; Lin et al., 2012; Song et al., 2016; Tang et al.,
113 2016; Chen, 2017b; Zhao et al., 2020), which were characterized by high levels in the heating period and low levels
114 in summer.

115 The heating period in North China was from November to March. Coal burning was used to be the major source for
116 heating in the NCP, but it has been gradually substituted by natural gas since 2013 in urban areas. In the rural areas,
117 however, there was still burning of coal and wood for heating. The emissions of SO₂ and NO_x in the heating period
118 were higher than those in the non-heating periods. Compared with the non-heating period, lower temperature, drier
119 air, weaker solar radiation, less precipitation, and lower mixing depth heights were found in the heating period,
120 resulting in lower atmospheric chemical reaction rate of SO₂ and NO_x, smaller removal effect of precipitation,
121 weaker vertical diffusion, longer atmospheric lifetime, and thus higher concentrations.

122 **3.3 Diurnal variations**

123 The average diurnal variations in SO₂ and NO_x mixing ratios at SDZ in different seasons are shown in Fig. 4. The
124 SO₂ mixing ratios peaked at 11:00 in spring and summer, 14:00 in fall, and 21:00 in winter. The NO_x mixing ratios
125 peaked at 1:00 in winter, 2:00 in spring, fall and summer. In addition, the valley of SO₂ diurnal cycle appeared at
126 5:00 in spring and summer, 6:00 in fall and winter, whereas for NO_x it was at 12:00 in spring, 13:00 in summer,
127 13:00 in fall, and 12:00 in winter, respectively. The diurnal behaviors of NO_x and SO₂ mixing ratios are different.
128 Generally, the average daily amplitudes of SO₂ are 3.0 ppb in spring, 2.0 ppb in summer, 4.4 ppb in fall, and 3.7 ppb
129 in winter, respectively, while the average daily amplitudes of NO_x are 6.8 ppb in spring, 6.3 ppb in summer, 10.6
130 ppb in fall and 10.5 ppb in winter, respectively.

131 3.4 Long-term trends of SO₂ and NO_x mixing ratios

132 Figure 5a shows the annual mean SO₂ mixing ratios from 2004 to 2016 at SDZ site, as well as the annual SO₂
133 emissions in North China (including Beijing, Tianjin, Hebei, Shanxi and Inner Mongolia). The annual mean SO₂
134 mixing ratio in 2004 was from Meng et al. (2009a). The SO₂ emission peaked in 2006 and then decreased with years.
135 Meanwhile, the annual mean SO₂ mixing ratio reached a high level around 7.6 ppb during 2006-2008, and then
136 began to decline thereafter. A rebound in SO₂ emission occurred in 2011, while a lagged rise of SO₂ mixing ratio
137 occurred in 2012. Overall, the annual mean SO₂ exhibited a significant decreasing trend of $-0.36 \text{ ppb yr}^{-1}$ (-6.1% yr
138 $^{-1}$, $R = -0.84$, $P < 0.01$) from 2004 to 2016 and a greater decreasing trend of $-0.56 \text{ ppb yr}^{-1}$ (-7.4% yr⁻¹, $R = -0.95$,
139 $P < 0.01$) from 2008 to 2016.

140 Figure 5b shows the long-term variations in the annual 5th and 95th percentile values of the hourly mean and annual
141 median of SO₂ mixing ratios in different years. The 95th percentile indicated the influence of polluted air masses,
142 while the 5th percentile indicated the influence of clean air masses. Similar to the trends of annual mean SO₂ mixing
143 ratios, the 95th percentile of SO₂ reached its peak (30.87 ppb) in 2007, and a little decrease in 2008 (29.19 ppb).
144 After 2008, it began to decline. Compared with the SO₂ level in 2008, there was a great decrease (-19.8%) in 2009,
145 but from 2009 to 2012 there was no significant decline in annual mean and annual median of SO₂. The most
146 significant downward trend of the 95th percentile of SO₂ was found from 2012 to 2016 with a rate of $-3.98 \text{ ppb yr}^{-1}$
147 (-16.3% yr⁻¹, $R = -0.99$, $P < 0.01$). However, the 5th percentile of SO₂ mixing ratios did not change significantly of
148 $-0.05 \text{ ppb yr}^{-1}$ (-2.6% yr⁻¹, $R = -0.15$, $P = 0.6$) from 2005 to 2016.

149 The annual mean of NO_x shows an increasing trend of $+0.37 \text{ ppb yr}^{-1}$ ($+3.4 \%$ yr⁻¹, $R = 0.38$, $P = 0.40$) from 2005 to
150 2010 with strong fluctuations (Fig. 5c,d). The annual NO_x mean reached the peak value (16.93 ppb) in 2010, and
151 exhibited a significant downward trend of $-0.77 \text{ ppb yr}^{-1}$ (-4.5% yr⁻¹, $R = 0.95$, $P < 0.01$) from 2010 to 2016 (Fig.
152 5c). The 95th percentile of the hourly mean of NO_x firstly increased during 2005-2012 with $+0.02 \text{ ppb yr}^{-1}$ ($+0.1 \%$
153 yr⁻¹, $R = 0.73$, $P < 0.05$) and then decreased during 2012-2016 with $-0.03 \text{ ppb yr}^{-1}$ (-4.7% yr⁻¹, $R = 0.95$, $P < 0.05$).
154 Similar to SO₂, the annual 5th percentile of NO_x mixing ratios did not change significantly (-1.7% yr⁻¹, $R = -0.18$,
155 $P = 0.58$) from 2005-2016 (Fig. 5d).

156 We regrouped NO_x and SO₂ data into 4 subsets according to the heating period (November-March), spring
157 (April-May), summer (June-August), and autumn (September-October). The long-term trends of the four subsets
158 are shown in Fig. 6. The SO₂ mixing ratios showed significant downward trends of $-0.96 \text{ ppb yr}^{-1}$ (-8.0% yr⁻¹, $R =$
159 -0.99 , $P < 0.01$) in the heating period, $-0.39 \text{ ppb yr}^{-1}$ (-5.2% yr⁻¹, $R = -0.84$, $P < 0.01$) in spring, $-0.24 \text{ ppb yr}^{-1}$

160 $(-4.3 \text{ \% yr}^{-1}, R = -0.92, P < 0.01)$ in autumn, and $-0.18 \text{ ppb yr}^{-1} (-7.7 \text{ \% yr}^{-1}, R = -0.87, P < 0.01)$ in summer. The
161 large reduction in the SO_2 level in the heating period was largely related to burning natural gas instead of coal for
162 domestic heating (Qiu et al., 2017; Li et al., 2020).

163 Except for autumn, the trends of the annual mean NO_x mixing ratios in other seasons showed a similar pattern that
164 NO_x mixing ratio rose firstly and then declined significantly. The annual mean of NO_x in autumn showed a
165 downward but statistically insignificant trend of $-0.08 \text{ ppb yr}^{-1} (-0.6 \text{ \% yr}^{-1}, R = -0.28, P = 0.38)$ from 2005 to
166 2016. In other seasons, the peaks of NO_x appeared in different years. The NO_x mixing ratios showed significant
167 downward trends of $-1.16 \text{ ppb yr}^{-1} (-5.4 \text{ \% yr}^{-1}, R = -0.84, P < 0.05)$ in the heating period during 2012–2016, -1.07
168 $\text{ppb yr}^{-1} (-7.6 \text{ \% yr}^{-1}, R = -0.96, P < 0.01)$ in spring during 2012–2017, and $-0.67 \text{ ppb yr}^{-1} (-4.5 \text{ \% yr}^{-1}, R = -0.87,$
169 $P = 0.01)$ in summer during 2011–2016.

170 **4 Discussion**

171 **4.1 The influence of emission control on long-term trends of NO_x and SO_2**

172 The annual mean and the 95th percentile of SO_2 mixing ratios at SDZ from 2004 to 2016 were significantly
173 correlated with the annual SO_2 emissions in North China with correlation coefficients of 0.85 ($P < 0.01$) and 0.88 (P
174 < 0.01), respectively. The decreasing rates of annual mean and 95th percentile of SO_2 mixing ratios from 2004 to
175 2016 at SDZ were -6.1 \% yr^{-1} and -6.2 \% yr^{-1} , respectively, which were higher than the trend (-3.1 \% yr^{-1}) of the
176 annual SO_2 emission in the NCP, but very close to the trend (-6.3 \% yr^{-1}) of the annual SO_2 emission in Beijing.
177 This indicated that surface SO_2 mixing ratios at SDZ were more influenced by the emission in Beijing than other
178 provinces in the NCP.

179 There seemed a lag between the variation of SO_2 mixing ratios and the emissions (Fig. 5a,b; Fig. S1a,b) and surface
180 SO_2 mixing ratio in 2012 was evidently inconsistent with the emission trend, which indicated the complexity of the
181 effect of reducing SO_2 emission on SO_2 mixing ratios. The effectiveness and timing of pollution control policies, as
182 well as the change of meteorology year by year, would cause their asynchronous trends. China has implemented a
183 series of stringent clean air actions from 2013 to 2017, and the “*Beijing 2013-2017 Clean Air Action Plan*” was
184 the most comprehensive and systematic pollution control program in Beijing (UN Environment, 2019). Before
185 2013, there would be some emissions being not counted for some reasons by local government, as the change
186 in the 95% percentile of SO_2 mixing ratios did not show a similar decreasing trend of the mean SO_2 mixing
187 ratios from 2009 to 2011. Another reason would be the change in SO_2 mixing ratios at the SDZ regional

188 background site was not as obvious as the change in Beijing urban and other polluted areas as Lin et al. (2012)
189 had stated. Changes in meteorology would also lead to a decoupling of emissions and measured SO₂ and NO₂
190 values, but it cannot be quantified how much the changes contributed to this time shift.

191 Taking 2008 as the base year, a stronger decreasing trend of $-7.4\% \text{ yr}^{-1}$ ($R = -0.95$, $P < 0.01$) from 2008 to 2016 for
192 the annual mean SO₂ mixing ratio can be found, as well as a significant decreasing rate of $(-4.5\% \text{ yr}^{-1}$, $R = -0.81$, P
193 < 0.01) for the annual 5 % percentile of SO₂ mixing ratios. More strict emission control measures had been
194 implemented for the 2008 Beijing Olympic Games, where the SO₂ pollution control had long-term effects and
195 benefits as Lin et al. (2012) had pointed out. Surface SO₂ mixing ratios in Beijing in the first half year of 2008
196 before the Olympic game, held in August and September, showed higher values than that in the rest of the year (Lin
197 et al., 2012). We believe the higher emission before the Olympics was due to more activities in preparing the
198 Olympic game. Although more reduction in SO₂ was seen in the post-Olympics period, the SO₂ mixing ratio showed
199 a higher annual mean in 2008 than in 2009. Theoretically, the worldwide economic crisis in 2009 might cause a
200 lower level of SO₂ but considering the economic stimulation measures implemented by the government, we do not
201 think the economic crisis played a significant role. Moreover, the higher NO_x emission in 2009 than in 2008
202 supports our view. The improvement of energy structure has been speeded up in Beijing from 2009, which might be
203 a more important factor. An assessment by the United Nations Environment Programme reported that the significant
204 decline in SO₂ mixing ratios and emissions from 1997–2017 was largely due to the SO₂ control measures in Beijing
205 and the surrounding areas, especially the transformation of coal-fired boilers, energy structure adjustments and the
206 end treatment of SO₂ tail gas (UN Environment, 2019). The SO₂ observation at SDZ background site confirmed the
207 effect of SO₂ reduction.

208 Before 2011, the annual mean NO_x showed an increasing trend with fluctuation year by year. There is a steep
209 increase in NO_x in 2010, as well as that in 2006. It is worth noting that the motor vehicles in Beijing in 2010 had
210 increased significantly from the previous year (see Figure S2), since the policy of purchase restriction in motor
211 vehicle was implemented in 2011. In addition, NO_x emissions from power plants and industrial sources were not
212 strictly controlled before 2011. Therefore, more NO_x would be emitted in years with prosperous economy.

213 According the analysis by Krotkov et al. (2016) and Duncan et al. (2016), NO₂ pollution over Northeast China has
214 reached its peak in 2011, and there have large decreases over Beijing, Shanghai, and the Pearl River Delta, which
215 were likely associated with local emission control efforts. Beijing has adopted the policy of "new car purchase
216 restriction" lottery number purchase since January 1, 2011 and has implemented the plan for further promoting the
217 elimination and renewal of old cars since August 1, 2011. New glass emission standard for air pollutants from the

218 flat glass industry (GB 26453-2011) was also implemented in this year. After 2010, the annual mean and 95th
219 percentile of NO_x mixing ratios correlated significantly ($R = 0.94, P < 0.01$ and $R = 0.82, P < 0.05$, respectively)
220 with the annual NO_x emission in North China, but the NO_x mixing ratios exhibited more fluctuations than NO_x
221 emissions (Fig. 5c, 5d). As shown in Fig. S1c and S1d, the annual mean NO_x mixing ratios were also significantly
222 correlated with the NO_x emission in Beijing ($R = 0.93, P < 0.01$) from 2010 to 2016 (Fig. S1c). However, the 95th
223 percentile of NO_x did not show a significant correlation ($R = 0.80, P = 0.06$) (Fig. S1d), indicating that high values
224 of NO_x at SDZ may be much more affected by NO_x emissions from other North China regions than Beijing. The
225 decreasing rates of $-4.8\% \text{ yr}^{-1}$ ($R = -0.92, P < 0.01$) for the annual mean and $-4.5\% \text{ yr}^{-1}$ ($R = -0.82, P < 0.05$) for
226 the 95th percentile NO_x mixing ratios from 2011 to 2016 at SDZ were lower than the one ($-8.8\% \text{ yr}^{-1}, R = -0.94, P$
227 < 0.01) for the annual NO_x emission in the NCP and ($-9.0\% \text{ yr}^{-1}, R = -0.96, P < 0.01$) in Beijing. Unlike the annual
228 mean or 95th percentile values, the 5th percentile of NO_x mixing ratios from 2011 to 2016 did not exhibit a
229 significant trend ($-5.0\% \text{ yr}^{-1}, R = -0.54, P = 0.27$) at SDZ.

230 It indicated that surface NO_x mixing ratios at SDZ was relatively weakly influenced by the emission reduction in
231 Beijing and its surrounding areas in the NCP compared with the condition of SO₂, probably because there were
232 more emission sources for NO_x than for SO₂. For example, although the coal-burning source pollution control
233 measures adopted in the *the Clean Air Action* have helped to reduce NO_x emissions, the increase in the amount of
234 motor vehicles led to an increase in NO_x emission from the traffic (Fontes et al., 2018; Sun et al., 2018; Zhang et al.,
235 2019; Zhang et al., 2020). In addition, the change of atmospheric transport conditions and the expansion of urban
236 scale may lead to the downward trend of NO_x, but not as obvious as that of SO₂ at SDZ (Lin et al., 2012).
237 Fortunately, NO_x pollution control measures on coal-burning source and vehicle pollution had also begun to achieve
238 more significant outcome since 2011 (Krotkov et al., 2016; UN Environment, 2019). Especially, vehicle pollution
239 control was strengthened through the improvement of oil quality and promotion of new energy vehicles. As a result,
240 Beijing's motor vehicle growth rate decreased from 19.7 % in 2010 to 3.6 % in 2011 and the number of new energy
241 vehicles had an increase of 431 % from 2013 to 2016 (Figure S2).

242 4.2 Variations in NO_x and SO₂ mixing ratios in different periods

243 We regrouped the NO_x and SO₂ data into 4 subsets in 4 different time stages (Stage I: 2005–2008, Stage II:
244 2009–2012, Stage III: 2013–2014, and Stage IV: 2015–2017). Key pollution control measures had been
245 implemented in different stages, e.g., emission controls for the 2008 Beijing Olympic Games, *the State Council Air*
246 *Pollution Prevention and Control Action Plan (Action Plan 2013–2017)* and *Beijing 2013–2017 Clean Air Action*

247 *Plan*. Details of the pollution prevention plans and its implementation can be found in UN Environment (2019) and
248 in Zheng et al. (2018), in which, control process and specific measures for coal combustion and motor vehicles in
249 Beijing from 1998 to 2017, and China's clean air policies implemented during 2010–2017 had been reviewed. Since
250 2015, the government of Beijing–Tianjin–Hebei region has promoted the application of electric energy substitution
251 using electric energy instead of traditional fossil energy (Wang et al., 2020).

252 The average diurnal variations in SO₂ and NO_x at SDZ in four stages are shown in Fig. 7 and Fig. S3. The SO₂ levels
253 and their amplitudes of the average diurnal variation continued to decrease as the stage time went by. The
254 differences in SO₂ among the 4 different periods are significant ($P < 0.001$) from the One-Way ANOVA test, and the
255 differences between the two groups are also significant ($P < 0.01$) from t-test. The diurnal amplitude of SO₂ was 4.16
256 ppb in Stage I and 0.94 ppb in Stage IV. The peak time of SO₂ in Stage IV appeared at 11:00 instead of the former
257 16:00. The peak value decreased significantly, from 9.38 ppb in Stage I to 3.19 ppb in Stage IV, with a factor of
258 –66.0 %. This phenomenon indicated that the control measures implemented in the period 2013–2017 have not only
259 had notable effects in reducing emissions from power plants, but also had significant achievement in the emission
260 control of non-electric industries such as industrial boilers and kilns (Zhang et al., 2019), which made the emission
261 intensity of SO₂ pollutants from elevated sources weaker than that in the Stage I.

262 Different from SO₂, the average diurnal of NO_x mixing ratios did not show a gradual decrease over time and with
263 values of Stage II > Stage III > Stage I > Stage IV. For NO_x, the differences among the 4 different periods are
264 significant ($P = 0.01$) from the One-Way ANOVA test, but the differences between the two groups are only significant
265 ($P < 0.01$) between Y2009-2012 and Y2015-2017 from t-test. In addition, the diurnal variations and the diurnal
266 amplitude of NO_x did not change much with the daily amplitudes being about 8.52 ppb. The peak and valley
267 appeared respectively at about 2:00 and at about 13:00 in 4 stages. The increase of NO_x and the decreasing of SO₂ in
268 Stage II tells the fact of much more effective of pollution control measures on SO₂ rather than NO_x implemented in
269 Beijing and other places. China intensified its acid rain control in the beginning of this century by much more strict
270 control of SO₂ emissions from coal-fired power plants. However, the control of NO_x emissions remained weak until
271 the introduction of the new Emission Standard of Air Pollutants for Thermal Power Plants (GB13223-2011) (Wang
272 et al., 2019). Such major difference in SO₂ and NO_x emission control caused an earlier peak for SO₂ (around 2006)
273 and a later peak for NO_x (around 2011-2012) (Li et al., 2017). The emission data for North China (Figure 5) nearly
274 resemble the nationwide situation and the mixing ratio data at SDZ (Figure 7) are consistent with the general trends
275 of SO₂ and NO_x emissions. At the same time, the amount of motor vehicles has been rapidly increasing, resulting in
276 an increase in NO_x emissions from vehicle exhaust.

277 Figure 8 shows the rose maps of SO₂ and NO_x mixing ratios in 4 different time periods (Figure S4 and S5 are rose
278 maps in different seasons, Table S1 is frequency distributions of wind directions in different stages). High NO_x
279 values were in broader wind sectors except NW–NNW–N–NNE, whereas high SO₂ values were mainly in
280 W–WSW–SW–SSW sectors. Except for the SSW sector, SO₂ mixing ratios in other wind directions showed a
281 decreasing trend over stages. Both the severely polluted areas and the slightly polluted areas have the same
282 characteristics of decreasing in SO₂ level over time (Table 3). Unlike the highest SO₂ mixing ratio being in Stage I
283 (2005–2008), the highest NO_x mixing ratios was in Stage II (2009–2012). The overall levels of SO₂ and NO_x in the
284 Stage IV reached the lowest values among the four stages. Compared with those at the stage with the highest mixing
285 ratios of NO_x and SO₂, the reduction ranges in Stage IV are 52.2 %–76.4 % for SO₂ and 3.8 %–45.3 % for NO_x in
286 different wind sectors. Much more reduction in SO₂ than NO_x indicates that the electric energy substitution policy in
287 Beijing–Tianjin–Hebei region has been much more effective on SO₂ reduction than NO_x.

288 The SO₂/NO_x ratio, obtained from the reduced major axis regression of the daily mean SO₂ and NO_x mixing ratios,
289 exhibited a significant change from 0.84 during 2005–2008 to 0.30 during 2015–2017. The possible reason for this
290 phenomenon was that the control measures including the upgrading of end treatment facilities of coal-fired power
291 plants, the conversion of coal to clean energy, and the elimination of coal-fired boilers, which were taken in the early
292 stage of *the Clean Air Action*, had greatly reduced SO₂ emissions rather than NO_x. Another reason could be an
293 increase in the number of motor vehicles (Figure S2) and relatively more difficulties in emission control on the
294 mobile sources. Unlike emissions from industries, emissions from automobiles are relatively more difficult to
295 control. The reason that supports this argument is that emissions from industrial plants could be quantitatively
296 measured, thus control measures that require a reduction of a certain percentage in emissions could be implemented.
297 However, the estimation of emissions from automobiles bears large uncertainties in the first place. Though there are
298 also strict control regulations as to cars with license plates of a chosen number are not allowed to be on road on
299 certain days, the actual reduction in emissions also depends on the usage of other cars.

300 In the period of 2005–2012, the construction of new power plants and the amount of motor vehicle ownership
301 rapidly increased in the city. During this period, flue gas desulfurization devices have been widely used (Zhao et al.,
302 2008). However, the main management measures that required power plants to deploy denitrification devices for
303 reducing NO_x emissions, have not been implemented until 2012, resulting in the increase of nitrogen oxide
304 emissions (Wang et al., 2010; Wang and Hao, 2012; Liu et al., 2016), and the contribution to the transport of NO_x to
305 SDZ during this period.

306 **4.3 The different diurnal behaviors in SO₂ and NO_x mixing ratios and their source origin**

307 The seasonal variations in SO₂ and NO_x mixing ratios exhibited a similar pattern with high values in winter and low
308 values in summer, and their daily mean values had a significant correlation ($R = 0.59$, $P < 0.01$). However, the
309 diurnal variations in SO₂ and NO_x mixing ratios were greatly different from each other (Figure 9). Due to the
310 increased emissions, lower mixing depth and slower chemical conversions in winter, SO₂ values showed significant
311 diurnal behavior in winter which was different from other seasons. Except for the winter, the SO₂ mixing ratios were
312 higher during the daytime and lower during the nighttime in all seasons, while the NO_x mixing ratios showed an
313 opposite pattern. The different diurnal behaviors in SO₂ and NO_x at SDZ might indicate a different origin of SO₂ and
314 NO_x.

315 Due to the diurnal variation in the boundary layer, the mixing depth is higher during the daytime and the convective
316 mixing is strong, which is conducive to the dilution and diffusion of pollutants. The photochemical reaction during
317 the daytime is also conducive to the chemical transformation of pollutants. At night, the pollutants are easy to
318 accumulate because of lower mixing depth and no photochemical processes. Therefore, the concentration of primary
319 pollutants exhibits higher values during the nighttime and lower during the daytime in general. But the situation for
320 SO₂ at SDZ was different. The higher SO₂ mixing ratios during the daytime suggested two possible mechanisms: (1)
321 an elevated level of SO₂ aloft, which could be mixed downward to the ground due to the evolution of atmospheric
322 boundary layer, causing higher ground-level SO₂ concentrations in the daytime. (2) upwind SO₂ sources and
323 transport of plumes in the daytime.

324 Since the SDZ station is selected as WMO/GAW regional station, local anthropogenic emissions are well avoided.
325 As SDZ is located on the north side of a valley with a northeast-southwest orientation, its dominant wind directions
326 were from southwest and northeast with regular changes in diurnal wind directions (Figure S6). The southwest
327 mouth of the valley is open to the NCP, so it is easily influenced by the air masses from the south polluted areas,
328 like urban Beijing. As a result, the concentration rose maps of pollutants exhibited higher values in the southwest
329 sectors than other sectors (Lin et al., 2008; Meng et al., 2009a). If only due to the influence by advection transport,
330 the diurnal variations in SO₂ and NO_x at SDZ should be similar. However, the two show obvious differences. The
331 higher SO₂ mixing ratios during the daytime indicates an elevated level of SO₂ in a high air layer, which can be
332 exchanged to the surface under the evolution of atmospheric boundary layer, causing a higher SO₂ value in the
333 daytime. The ‘unusual’ phenomenon of the diurnal change in SO₂ has been noticed and explained by studies (Lin et
334 al., 2008; Chen et al., 2009; Xu et al., 2014), but it lacked direct vertical profile measurements to support this

335 explanation. The daytime peak of SO₂ was not only found at SDZ, but also at different sites in urban and rural areas
336 in North China (Lin et al., 2012) and in the background area of the Yangtze River Delta (Qi et al., 2012). This may
337 be related to the fact that SO₂ is mainly emitted from elevated sources (Lin et al., 2012; Xu et al., 2014). The daily
338 maximum of SO₂ concentrations was caused by the downward mixing of SO₂ emitted by elevated sources in this
339 region. As strict and effective control measures were continuously implemented, the contribution from such a source
340 largely decreased and finally became negligible. Governed by the development of the planetary boundary layer, the
341 diurnal variation of SO₂ concentrations would peak around noon. This may be the cause of the shift in time of the
342 SO₂ maximum as mentioned in Section 4.2. Xu et al. (2014) have discussed the implications of this SO₂
343 noontime-peak phenomenon in sulphur deposition and transformation. At night, prevail north wind transported clean
344 air to SDZ. This process should be the major cause of the decreasing SO₂ levels during nighttime, since surface SO₂
345 mixing ratios depend on vertical air exchange. Enhanced relative humidity during nighttime should be also a loss
346 effect since SO₂ is a very soluble gas. In addition, dry deposition of SO₂ in a shallow nocturnal boundary layer
347 might lower the SO₂ level as well.

348 It can be seen that the NO_x mixing ratios began to rise around noontime when the mixing depth was still elevating
349 (Figure 9). Obviously, NO_x was affected by the transport of pollutants in the southern polluted area during the
350 noontime when the WD changed into southwest wind (Figure S6). Of course, motor vehicles running on the roads
351 and dispersing human activities can emit NO_x as well as the transport from the south. As seen in Figure 8, the NO_x
352 rose map showed wider source origins than SO₂. However, SO₂ maintained a relatively high value instead of
353 increasing significantly, indicating that SO₂ mixing ratios were still mainly affected by downward mixing of
354 SO₂-richer air.

355 **Conclusion**

356 Measurements of surface NO_x and SO₂ mixing ratios at SDZ regional atmospheric background site in the North
357 China Plain from the period 2005–2017, together with ancillary data, were summarized and used to study their
358 long-term trends and influencing factors. The average values $\pm 1\sigma$ (standard deviation) of SO₂ and NO_x mixing
359 ratios were 5.7 ± 8.4 ppb and 14.2 ± 12.4 ppb, respectively. The seasonal variation in SO₂ and NO_x at SDZ showed a
360 similar pattern with high values in winter and low values in summer, but the diurnal variations in SO₂ and NO_x
361 mixing ratio exhibited large differences in all seasons. The SO₂ mixing ratios were higher during the daytime and
362 lower during the nighttime, while the NO_x mixing ratios showed higher values during the nighttime and lower

363 during the daytime. The different diurnal behaviors in SO₂ and NO_x at SDZ indicated a different origin of SO₂ and
364 NO_x.

365 Overall, the annual mean SO₂ exhibited a significant decreasing trend of $-0.36 \text{ ppb yr}^{-1}$ ($-6.1 \% \text{ yr}^{-1}$, $R = -0.84$, $P <$
366 0.01) from 2004 to 2016 and a greater decreasing trend of $-0.56 \text{ ppb yr}^{-1}$ ($-7.4 \% \text{ yr}^{-1}$, $R = -0.95$, $P < 0.01$) from
367 2008 to 2016. The decreasing rates of annual mean and 95th percentile of SO₂ mixing ratios from 2004 to 2016 at
368 SDZ are very close to the one ($-6.3 \% \text{ yr}^{-1}$) of the annual SO₂ emission in Beijing. The annual mean of NO_x showed
369 a fluctuating rise of $+0.37 \text{ ppb yr}^{-1}$ ($+3.4 \% \text{ yr}^{-1}$, $R = 0.38$, $P = 0.40$) from 2005 to 2010, reaching the peak value
370 (16.93 ppb) in 2010, and then exhibited an extremely significant fluctuating downward trend of $-0.77 \text{ ppb yr}^{-1}$
371 ($-4.5 \% \text{ yr}^{-1}$, $R = 0.95$, $P < 0.01$) from 2010 to 2016. After 2010, the annual mean and 95 % percentile of NO_x
372 mixing ratios correlated significantly ($R = 0.94$, $P < 0.01$ and $R = 0.82$, $P < 0.05$, respectively) with the annual NO_x
373 emission in North China. The decreasing rates of $-4.8 \% \text{ yr}^{-1}$ ($R = -0.92$, $P < 0.01$) for the annual mean and -4.5%
374 yr^{-1} ($R = -0.82$, $P < 0.05$) for the 95th percentile NO_x mixing ratios from 2011 to 2016 at SDZ are lower than the
375 one ($-8.8 \% \text{ yr}^{-1}$, $R = -0.94$, $P < 0.01$) for the annual NO_x emission in the NCP and ($-9.0 \% \text{ yr}^{-1}$, $R = -0.96$, $P <$
376 0.01) in Beijing. It indicated that surface NO_x mixing ratios at SDZ had a weaker response to the emission reduction
377 in Beijing and its surrounding areas in NCP than SO₂. The increase in the amount of motor vehicles and the weak
378 effectiveness of traffic restrictions have caused motor vehicle emissions on NO_x.

379 **Data availability.** The data in this study can be publicly accessed via <https://doi.org/10.7910/DVN/YFVLHV> (Liu et
380 al., 2022).

381 **Author contributions.** XL wrote the paper, WL developed the idea, formulated the research goals, and edited the
382 paper. LR, XX and ZQ edited the paper. WL, FD, DH, LZ, QS and YW carried out the measurement of NO_x and
383 SO₂, and analysed the meteorological data.

384 **Competing interests.** The authors declare that they have no conflict of interest.

385 **Acknowledgements.** This study was funded by the National Natural Science Foundation of China (Grant No.
386 91744206) and the Open Fund of Shangdianzi Atmospheric Background Station (SDZ2020615).

387 **References**

- 388 Bai, J., Wu, Y., Chai, W., Wang, P., and Wang, G.: Long-term variation of trace gases and particulate matter at an atmospheric
389 background station in North China (in Chinese), *Advances in Geosciences.*, 5, 248-263,
390 <https://doi.org/10.12677/AG.2015.53025>, 2015.
- 391 Cai, K., Zhang, Q., Li, S., Li, Y., and Ge, W.: Spatial-temporal variations in NO₂ and PM_{2.5} over the Chengdu–Chongqing
392 economic zone in China during 2005 – 2015 based on satellite remote sensing, *Sensors-Basel.*, 18, 3950,
393 <https://doi.org/10.3390/s18113950>, 2018.
- 394 Chen, L.: Measure and study on the atmospheric pollutants in three typical regional background stations of China (in Chinese),
395 Master, Lanzhou University, 2012.
- 396 Chen, T., Chang, K., and Tsai, C.: Modeling approach for emissions reduction of primary PM_{2.5} and secondary PM_{2.5} precursors
397 to achieve the air quality target, *Atmos. Res.*, 192, 11-18, <https://doi.org/10.1016/j.atmosres.2017.03.018>, 2017a.
- 398 Chen, C.: Analysis of atmospheric pollutants characteristics in the typical suburban station of North China (in Chinese), Master,
399 Nanjing University of Information Science and Technology, 2017b.
- 400 Chen, Y., Zhao, C., Qiang, Z., Deng, Z., Huang, M., and Ma, X.: Aircraft study of mountain chimney effect of Beijing, China, *J.*
401 *Geophys. Res-atmos.*, 114, D8306, <https://doi.org/10.1029/2008JD010610>, 2009.
- 402 Cheng, M., Pan, Y., Wang, H., Liu, Q., and Wang, Y.: On-line measurement of water-soluble composition of particulate matter
403 in Beijing (in Chinese), *Environ. Sci.*, 34, 2943-2949, <https://doi.org/10.13227/j.hjx.2013.08.018>, 2013,
- 404 Cheng, N., Chen, T., Zhang, D., Li, Y., Sun, F., Wei, Q., Liu, J., Liu, B., and Sun, R.: Air quality characteristics in Beijing during
405 Spring Festival in 2015 (in Chinese), *Environ. Sci.*, 36, 3150-3158, <https://doi.org/10.13227/j.hjx.2015.09.005>, 2015.
- 406 Cheng, L., Ji, D., He, J., Li, L., Du, L., Cui, Y., Zhang, H., Zhou, L., Li, Z., and Zhou, Y.: Characteristics of air pollutants and
407 greenhouse gases at a regional background station in Southwestern China, *Aerosol Air Qual. Res.*, 19, 1007-1023,
408 <https://doi.org/10.4209/aaqr.2018.11.0397>, 2019.
- 409 Fontes, T., Li, P., Barros, N., and Zhao, P.: A proposed methodology for impact assessment of air quality traffic-related measures:
410 The case of PM_{2.5} in Beijing, *Environ. Pollut.*, 239, 818-828, <https://doi.org/10.1016/j.envpol.2018.04.061>, 2018.
- 411 Gao, J., Zhang, Y., Wang, S., Chai, F., and Chen, Y.: Study on the characteristics and formation of a multi-day haze in October
412 2011 in Beijing (in Chinese), *Res. Environ. Sci.*, 25, 1201-1207, <https://doi.org/CNKI:SUN:HJKX.0.2012-11-002>, 2012.
- 413 Jung, J., Lee, J., Kim, B., and Oh, S.: Seasonal variations in the NO₂ artifact from chemiluminescence measurements with a
414 molybdenum converter at a suburban site in Korea (downwind of the Asian continental outflow) during 2015–2016, *Atmos.*
415 *Environ.*, 165, 290-300, <https://doi.org/10.1016/j.atmosenv.2017.07.010>, 2017.

416 Krotkov, N. A., Mclinden, C. A., Li, C., Lamsal, L. N., Celarier, E. A., Marchenko, S. V., Swartz, W. H., Bucsela, E. J., Joiner, J.,
417 and Duncan, B. N.: Aura OMI observations of regional SO₂ and NO₂ pollution changes from 2005 to 2015, *Atmos. Chem.*
418 *Phys.*, 16, 4605-4629, <https://doi.org/10.5194/acp-16-4605-2016>, 2016.

419 Li, F., Tan, H., Deng, X., Deng, T., Xu, W., Ran, L., and Zhao, C.: Characteristics analysis of sulfur dioxide in Pearl River Delta
420 from 2006 to 2010 (in Chinese), *Environ. Sci.*, 5, 1530-1537, <https://doi.org/CNKI:SUN:HJKZ.0.2015-05-003>, 2015.

421 Li, M., Liu, H., Geng, G., Hong, C., Liu, F., Song, Y., Tong, D., Zheng, B., Cui, H., Man, H., Zhang, Q. and He, K.:
422 Anthropogenic emission inventories in China: a review, *National Science Review*, 4, 834-866,
423 <https://doi.org/10.1093/nsr/nwx150>, 2017.

424 Li, Y., Wang, J., Han, T., Wang, Y., He, D., Quan, W., and Ma, Z.: Using multiple linear regression method to evaluate the
425 impact of meteorological conditions and control measures on air quality in Beijing during APEC 2014 (in Chinese), *Environ.*
426 *Sci.*, 40, 1024-1034, <https://doi.org/10.13227/j.hjkx.201807044>, 2019.

427 Li, W., Shao, L., Wang, W., Li, H., Wang, X., Li, Y., Li, W., Jones, T., and Zhang, D.: Air quality improvement in response to
428 intensified control strategies in Beijing during 2013 – 2019, *Sci. Total. Environ.*, 744, 140776,
429 <https://doi.org/10.1016/j.scitotenv.2020.140776>, 2020.

430 Lin, W., Xu, X., Zhang, X., and Tang, J.: Contributions of pollutants from North China Plain to surface ozone at the Shangdianzi
431 GAW station, *Atmos. Chem. Phys.*, 8, 5889-5898, <https://doi.org/10.5194/acp-8-5889-2008>, 2008.

432 Lin, W., Xu, X., Ge, B., and Zhang, X.: Characteristics of gaseous pollutants at Gucheng, a rural site southwest of Beijing, *J.*
433 *Geophys. Res-atmos.*, 114, D14G, <https://doi.org/10.1029/2008JD010339>, 2009a.

434 Lin, W., Xu, X., Yu, D., Dai, X., Zhang, Z., Meng, Z., and Wang, Y.: Quality control for reactive gases observation at
435 Longfengshan regional atmospheric background monitoring station (in Chinese), *Meteorol. Mon.*, 35, 93-100,
436 <https://doi.org/10.7519/j.issn.1000-0526.2009.11.012>, 2009b.

437 Lin, W., Xu, X., Ge, B., and Liu, X.: Gaseous pollutants in Beijing urban area during the heating period 2007–2008: variability,
438 sources, meteorological, and chemical impacts, *Atmos. Chem. Phys.*, 11, 6919-6959,
439 <https://doi.org/10.5194/acp-11-8157-2011>, 2011a.

440 Lin, W., Xu, X., Sun, J., Li, Y., and Meng, Z.: Background concentrations of reactive gases and the impacts of long-range
441 transport at the Jinsha regional atmospheric background station, *Sci. China Earth Sci.*, 54, 1604-1613,
442 <https://doi.org/10.1007/s11430-011-4205-2>, 2011b.

443 Lin, W., Xu, X., Ma, Z., Zhao, H., Liu, X., and Wang, Y.: Characteristics and recent trends of sulfur dioxide at urban, rural, and
444 background sites in North China: Effectiveness of control measures, *J. Environ. Sci.*, 24, 34-49,
445 [https://doi.org/10.1016/s1001-0742\(11\)60727-4](https://doi.org/10.1016/s1001-0742(11)60727-4), 2012.

446 Lin, W., Ma, Z., Pu, W., Gao, W., Ma, Q., and Yu, D.: Air Composition-Quality control for observation data-Reactive gases.
447 Meteorological industry Standard of the People's Republic of China (QX/T 510-2019), 2019.

448 Liu, J., Zhang, X., Xu, X., and Xu, H.: Comparison analysis of variation characteristics of SO₂, NO_x, O₃ and PM_{2.5} between rural
449 and urban areas, Beijing (in Chinese), *Environ. Sci.*, 29, 1059-1065, <https://doi.org/10.3321/j.issn:0250-3301.2008.04.036>,
450 2008.

451 Liu, R., Han, Z., and Li, J.: Analysis of meteorological characteristics during winter haze events in Beijing (in Chinese), *Clim.*
452 *Environ. Res.*, 19, 164-172, <https://doi.org/10.3878/j.issn.1006-9585.2014.13224>, 2014a.

453 Liu, X., Xu, X., Zhao, H., and Lin, W.: Characteristics of NO_x and CO emission on the three sites in Beijing and its surrounding
454 areas (in Chinese), *J. Saf. Environ.*, 14, 252-257, <https://doi.org/10.13637/j.issn.1009-6094.2014.06.056>, 2014b.

455 Liu, F., Zhang, Q., Van, D. A. R. J., Zheng, B., Tong, D., Yan, L., Zheng, Y., and He, K.: Recent reduction in NO_x emissions
456 over China: synthesis of satellite observations and emission inventories, *Environ. Res. Lett.*, 11, 3945-3950,
457 <https://doi.org/10.1088/1748-9326/11/11/114002>, 2016.

458 Luo, X., Pan, Y., Goulding, K., Zhang, L., Liu, X., and Zhang, F.: Spatial and seasonal variations of atmospheric sulfur
459 concentrations and dry deposition at 16 rural and suburban sites in China, *Atmos. Environ.*, 146, 79-89,
460 <https://doi.org/10.1016/j.atmosenv.2016.07.038>, 2016.

461 Meng, Z., Xu, X., Yan, P., Ding, G., Tang, J., Lin, W., Xu, X., and Wang, S.: Characteristics of trace gaseous pollutants at a
462 regional background station in Northern China, *Atmos. Chem. Phys.*, 9, 927-936, <https://doi.org/10.5194/acp-9-927-2009>,
463 2009a.

464 Meng, X., Wang, P., Wang, G., Yu, H., and Zong, X.: Variation and transportation characteristics of SO₂ in winter over Beijing
465 and its surrounding areas (in Chinese), *Clim. Environ. Res.*, 14, 83-91, <https://doi.org/10.3878/j.issn.1006-9585.2009.03.08>,
466 2009b.

467 Qi, H., Lin, W., Xu, X., and Yu, X.: Significant downward trend of SO₂ observed from 2005 to 2010 at a background station in
468 the Yangtze Delta region, China, *Sci. China. Chem.*, 55, 1451-7291, <https://doi.org/10.1007/s11426-012-4524-y>, 2012.

469 Qiu, X., Duan, L., Cai, S., Yu, Q., Wang, S., Chai, F., Gao, J., Li, Y., and Xu, Z.: Effect of current emission abatement strategies
470 on air quality improvement in China: A case study of Baotou, a typical industrial city in Inner Mongolia, *J. Environ.*
471 *Sci.-China.*, 57, 383-390, <https://doi.org/10.1016/j.jes.2016.12.014>, 2017.

472 Shao, M., Tang, X., Zhang, Y., and Li, W.: City clusters in China: air and surface water pollution, *Front. Ecol. Environ.*, 4,
473 353-361, [https://doi.org/10.1890/1540-9295\(2006\)004\[0353:CCICAA\]2.0.CO](https://doi.org/10.1890/1540-9295(2006)004[0353:CCICAA]2.0.CO), 2006.

474 Su, B., Liu, X., and Tao, J.: Pollution characteristics of SO₂, NO_x and CO in forest and mountain background region of East
475 China (in Chinese), *Environ. Monit. China.*, 29, 15-21, <https://doi.org/10.3969/j.issn.1002-6002.2013.06.004>, 2013.

476 Song, C., Li, R., Jianjun, H., Wu, L., and Mao, H.: Analysis of pollution characteristics of NO, NO₂ and O₃ at urban area of
477 Langfang, Hebei (in Chinese), *J. Environ. Sci.-China.*, 36, 2903-2912, <https://doi.org/CNKI:SUN:ZGHJ.0.2016-10-004>, 2016.

478 Steinbacher, M., Zellweger, C., Schwarzenbach, B., Bugmann, S., Buchmann, B., Ordóñez, C., Prevot, A. S. H., and Hueglin, C.:
479 Nitrogen oxide measurements at rural sites in Switzerland: Bias of conventional measurement techniques, *J. Geophys.*
480 *Res-atmos.*, 112(D11), <https://doi.org/10.1029/2006JD007971>, 2007.

481 Sun, C., Luo, Y., and Li, J.: Urban traffic infrastructure investment and air pollution: Evidence from the 83 cities in China, *J.*
482 *Clean. Prod.*, 172, 488-496, <https://doi.org/10.1016/j.jclepro.2017.10.194>, 2018.

483 Shikwambana, L., Mhangara, P., and Mbatha, N.: Trend analysis and first time observations of sulphur dioxide and nitrogen
484 dioxide in South Africa using TROPOMI/Sentinel-5 P data, *Int. J. Appl. Earth Obs. Geoinf.*, 91, 102130,
485 <https://doi.org/10.1016/j.jag.2020.102130>, 2020.

486 Tang, Y., Zhang, X., Xu, J., Zhao, X., Ma, Z., and Meng, W.: Multi-temporal scale variations of atmospheric pollutants
487 concentrations in rural and urban areas of Beijing (in Chinese), *Acta Sci. Circumst.*, 36, 2783-2793,
488 <https://doi.org/10.13671/j.hjkxxb.2016.0003>, 2016.

489 UN Environment. A Review of 20 Years' Air Pollution Control in Beijing. United Nations Environment Programme, Nairobi,
490 Kenya, 2019.

491 Wang, N., Lyu, X., Deng, X., Huang, X., Jiang, F., Ding, A.: Aggravating O₃ pollution due to NO_x emission control in eastern
492 China, *Science of the Total Environment*, 677, 732-744, <https://doi.org/10.1016/j.scitotenv>, 2019.

493 Wang, S., Streets, D. G., Zhang, Q., He, K., Chen, D., Kang, S., Lu, Z., and Wang, Y.: Satellite detection and model verification
494 of NO_x emissions from power plants in Northern China, *Environ. Res. Lett.*, 5, 44007,
495 <https://doi.org/10.1088/1748-9326/5/4/044007>, 2010.

496 Wang, S., and Hao, J.: Air quality management in China: Issues, challenges, and options, *J. Environ. Sci.*, 24, 2-13,
497 [https://doi.org/10.1016/S1001-0742\(11\)60724-9](https://doi.org/10.1016/S1001-0742(11)60724-9), 2012.

498 Wang, Y., Wang, S., Song, F., Yang, J., Zhu, J., and Zhang, F.: Study on the forecast model of electricity substitution potential in
499 Beijing – Tianjin – Hebei region considering the impact of electricity substitution policies, *Energ. Policy.*, 144, 111686,
500 <https://doi.org/10.1016/j.enpol.2020.111686>, 2020.

501 WMO. 2001. Global Atmosphere Watch Measurements Guide (WMO TD No. 1073). GAW Report No. #171. Geneva,
502 Switzerland: World Meteorological Organization. Accessed on April 2, 2015. Available at
503 <ftp://ftp.wmo.int/Documents/PublicWeb/arep/gaw/gaw143.pdf>.

504 Wu, D., Xin, J., Sun, Y., Wang, Y., and Wang, P.: Change and analysis of background concentration of air pollutants in North
505 China during 2008 Olympic Games (in Chinese), *Environ. Sci.*, 31, 1130-1138,
506 <https://doi.org/CNKI:SUN:HJKZ.0.2010-05-003>, 2010.

507 Xu, X., Lin, W., Yan, P., Zhang, Z., and Yu, X.: Long-term changes of acidic gases in China's Yangtze Delta and Northeast
508 Plain regions during 1994 – 2006 (in Chinese), *Adv. Clim. Chang. Res.*, 4, 195-201,
509 <https://doi.org/10.3969/j.issn.1673-1719.2008.04.001>, 2008.

510 Xu, X., Liu, X., and Lin, W.: Impacts of air parcel transport on the concentrations of trace gases at regional background stations
511 (in Chinese), *J. Appl. Meteorol. Sci.*, 20, 656-664, <https://doi.org/10.11898/1001-7313.20090602>, 2009.

512 Xu, W., Zhao, C., Ran, L., Lin, W., Yan, P., and Xu, X.: SO₂ noontime-peak phenomenon in the North China Plain, *Atmos.*
513 *Chem. Phys.*, 14, 7757-7768, <https://doi.org/10.5194/acp-14-7757-2014>, 2014.

514 Yang, S., Zhao, X., and Liu, N.: Impacting factors of a heavy air pollution process in autumn over Beijing (in Chinese), *J.*
515 *Meteorol. Environ.*, 13-16, <https://doi.org/10.3969/j.issn.1673-503X.2010.05.003>, 2010.

516 Yang, F., Tan, J., Zhao, Q., Du, Z., He, H., Ma, Y., Duan, F., Chen, G., and Zhao, Q.: Characteristics of PM_{2.5} speciation in
517 representative megacities and across China, *Atmos. Chem. Phys.*, 11, 1025-1051, <https://doi.org/10.5194/acp-11-5207-2011>,
518 2011.

519 Yin, Q., Ma, Q., Lin, W.*, Xu, X., and Yao, J.: Measurement report: Long-term variations in surface NO_x and SO₂ from 2006 to
520 2016 at a background site in the Yangtze River Delta region, China, *Atmos. Chem. Phys.*, 22, 1015–1033,
521 <https://doi.org/10.5194/acp-22-1015-2022>, 2022.

522 Zhang, X., Zhang, P., Zhang, Y., Li, X., and Qiu, H.: The trend, seasonal cycle, and sources of tropospheric NO₂ over China
523 during 1997–2006 based on satellite measurement, *Sci China Earth Sci.*, 50, 8, <https://doi.org/10.1007/s11430-007-0141-6>,
524 2007.

525 Zhang, Q., Zheng, Y., Tong, D., Shao, M., Wang, S., Zhang, Y., Xu, X., Wang, J., He, H., Liu, W., Ding, Y., Lei, Y., Li, J.,
526 Wang, Z., Zhang, X., Wang, Y., Cheng, J., Liu, Y., Shi, Q., Yan, L., Geng, G., Hong, C., Li, M., Liu, F., Zheng, B., Cao, J.,
527 Ding, A., Gao, J., Fu, Q., Huo, J., Liu, B., Liu, Z., Yang, F., He, K., and Hao, J.: Drivers of improved PM_{2.5} air quality in
528 China from 2013 to 2017, *P. Natl. Acad. Sci. Usa.*, 116, 24463-24469, <https://doi.org/10.1073/pnas.1907956116>, 2019.

529 Zhang, M., Shan, C., Wang, W., Pang, J., and Guo, S.: Do driving restrictions improve air quality: Take Beijing–Tianjin for
530 example? *Sci. Total Environ.*, 712, 136408, <https://doi.org/10.1016/j.scitotenv.2019.136408>, 2020.

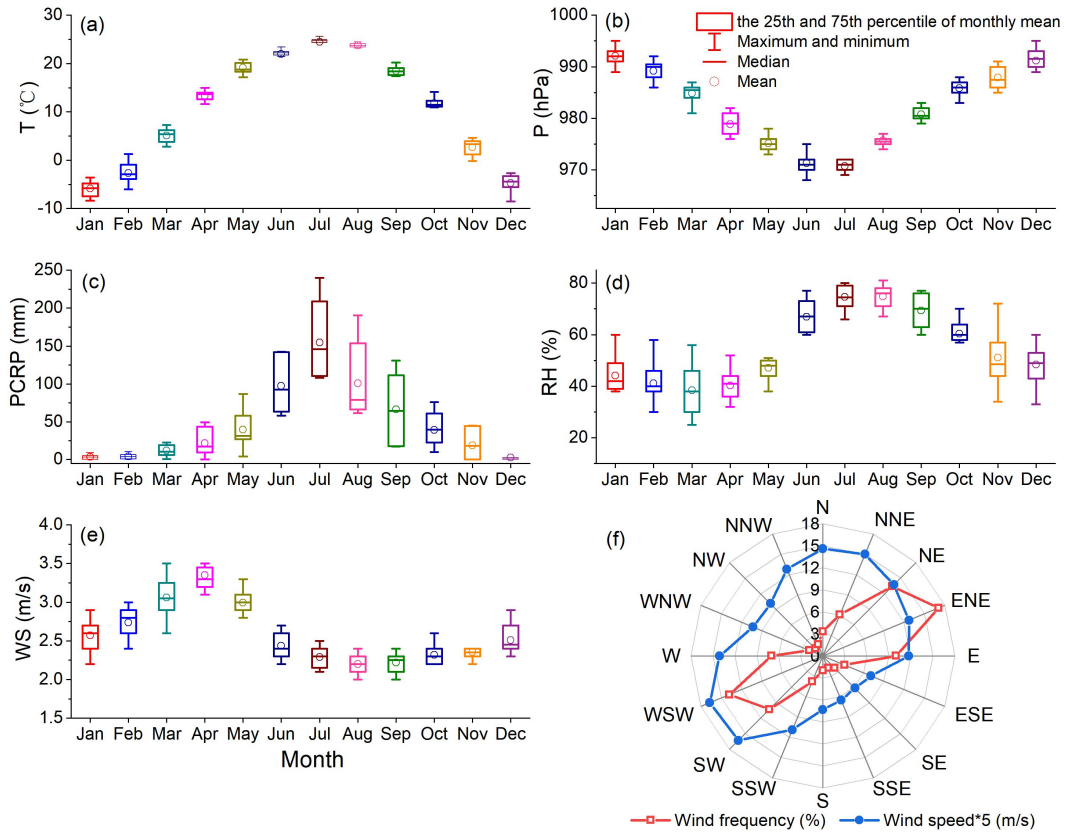
531 Zhao, Y., Wang, S., Duan, L., Lei, Y., Cao, P., and Hao, J.: Primary air pollutant emissions of coal-fired power plants in China:
532 Current status and future prediction, *Atmos. Environ.*, 42, 8442-8452, <https://doi.org/10.1016/j.atmosenv.2008.08.021>, 2008.

533 Zhao, P. S., Dong, F., D, H., Zhao, X. J., Zhang, X. L., Zhang, W. Z., Yao, Q., and Liu, H. Y.: Characteristics of concentrations
534 and chemical compositions for PM_{2.5} in the region of Beijing, Tianjin, and Hebei, China, *Atmos. Chem. Phys.*, 9, 4631-4644,
535 <https://doi.org/10.5194/acp-13-4631-2013>, 2013.

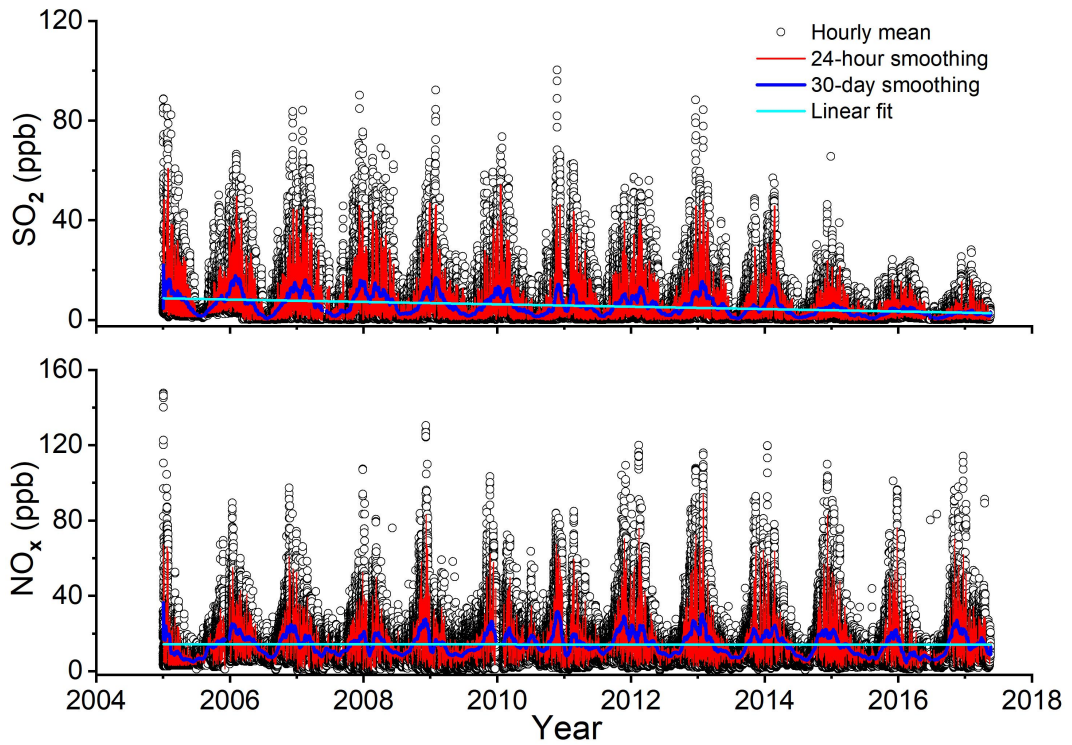
536 Zhao, S., Hu, B., Gao, W., Li, L., Huang, W., Wang, L., Yang, Y., Liu, J., Li, J., Ji, D., Zhang, R., Zhang, Y., and Wang, Y.:
537 Effect of the "coal to gas" project on atmospheric NO_x during the heating period at a suburban site between Beijing and
538 Tianjin, *Atmos. Res.*, 241, 104977, <https://doi.org/10.1016/j.atmosres.2020.104977>, 2020.

539 Zheng, B., Tong, D., Li, M., Liu, F., Hong, C., Geng, G., Li, H., Li, X., Peng, L., Qi, J., Yan, L., Zhang, Y., Zhao, H., Zheng, Y.,
540 He, K., and Zhang, Q.: Trends in China's anthropogenic emissions since 2010 as the consequence of clean air actions, *Atmos.*
541 *Chem. Phys.*, 18, 14095-14111, <https://doi.org/10.5194/acp-18-14095-2018>, 2018.

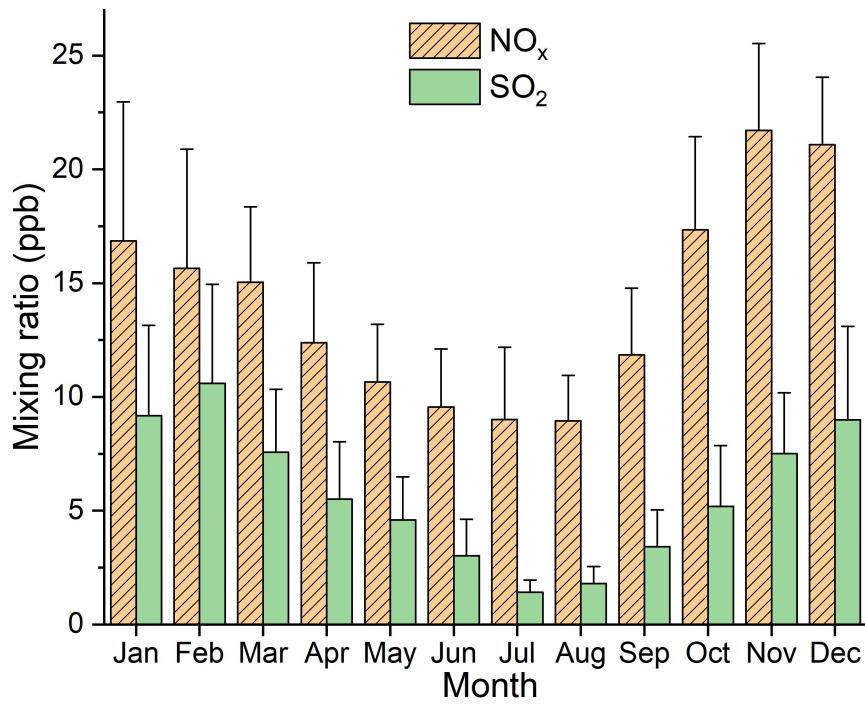
542 Zhong, Y., Zhou, Y., Cheng, S., Wang, X., and Shao, X.: Comparison analysis of the effect of emission reduction measures for
543 major events and heavy air pollution in the capital (in Chinese), *Environ. Sci.*, 41, 3449-3457,
544 <https://doi.org/10.13227/j.hjcx.201910166>, 2020.



545 **Figure 1.** Monthly variations in (a) air temperature. (b) atmospheric pressure. (c) precipitation. (d) relative humidity. (e) wind speed. (f) wind rose map. at SDZ.

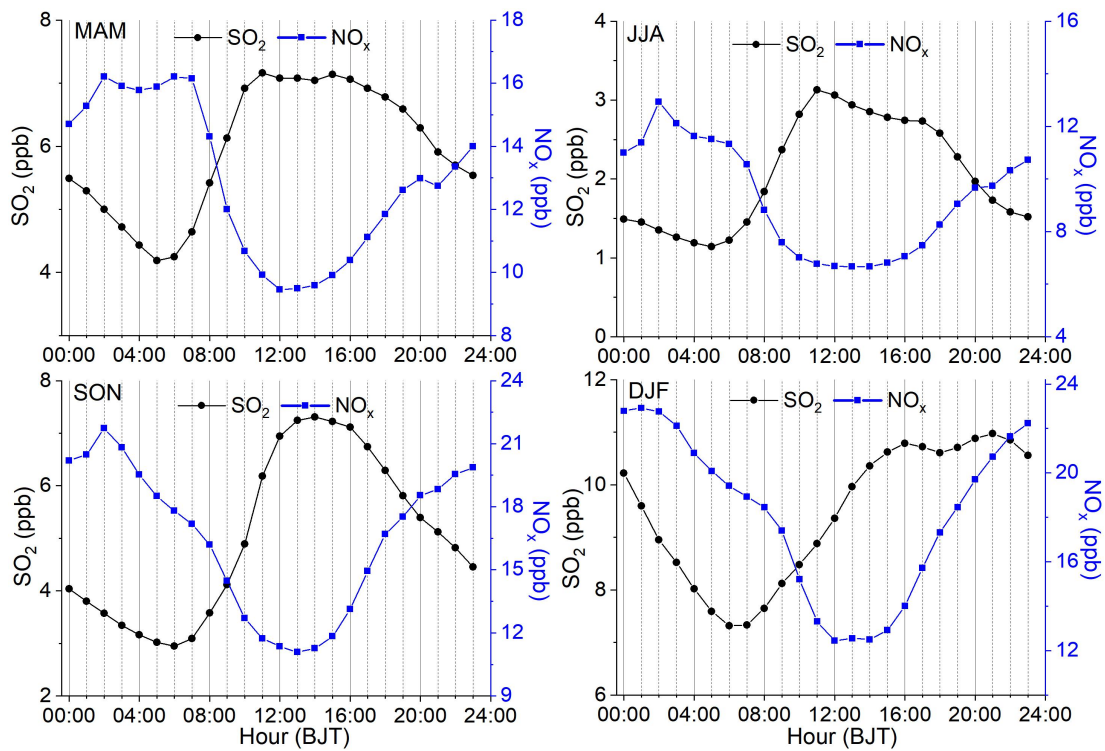


546 **Figure 2.** The time series variations in SO₂ and NO_x mixing ratios at SDZ.



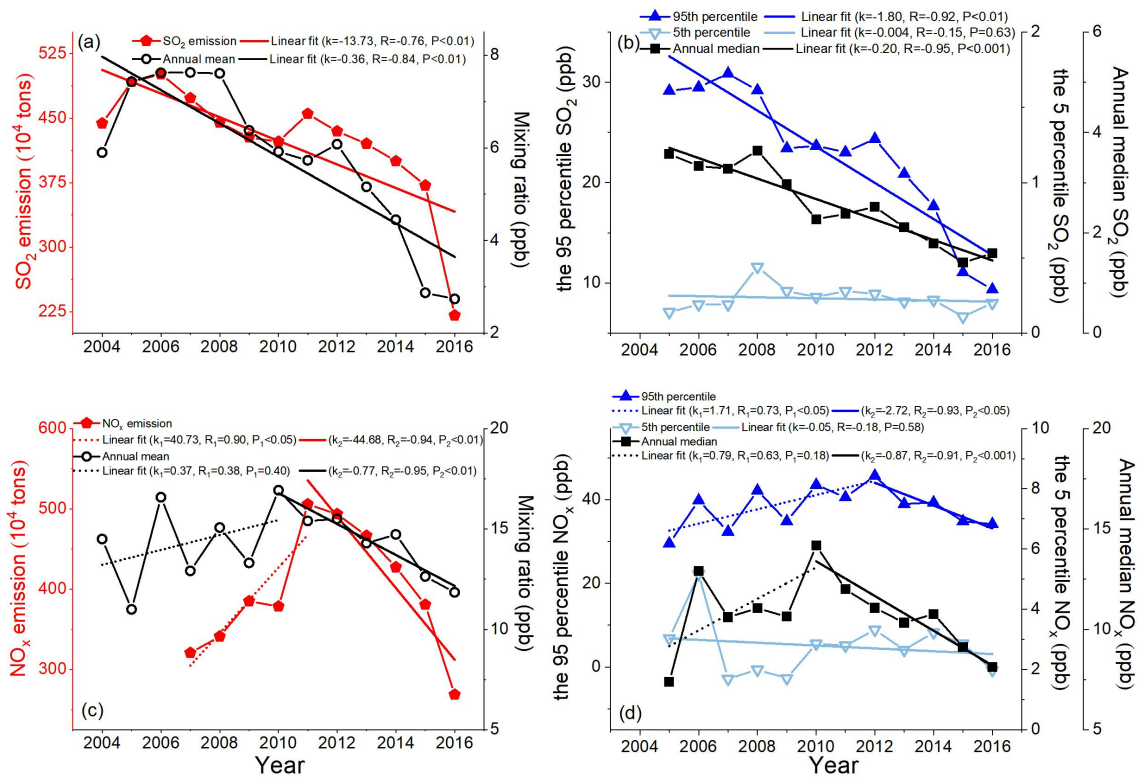
547

Figure 3. The average monthly mean of SO₂ and NO_x mixing ratios with 1 σ at SDZ.



548

Figure 4. The Average diurnal variations in SO₂ and NO_x mixing ratios in four seasons at SDZ.



549

Figure 5. Annually variations in (a) SO₂ mixing ratios at SDZ and total SO₂ emissions in North China; (b) the 5th and 95th percentile of the hourly mean and annual median of SO₂ mixing ratios and SO₂ emissions in North China; (c) NO_x mixing ratios at SDZ and total NO_x emissions in North China; (d) the 5th and 95th percentile of the hourly mean and annual median of NO_x mixing ratios and NO_x emissions in North China. The emission data are from the 2005–2017 Yearbook of National Bureau of Statistics of China and China Statistical Yearbook on Environment provided by Ministry of Ecology and Environment of the People's Republic of China.

550

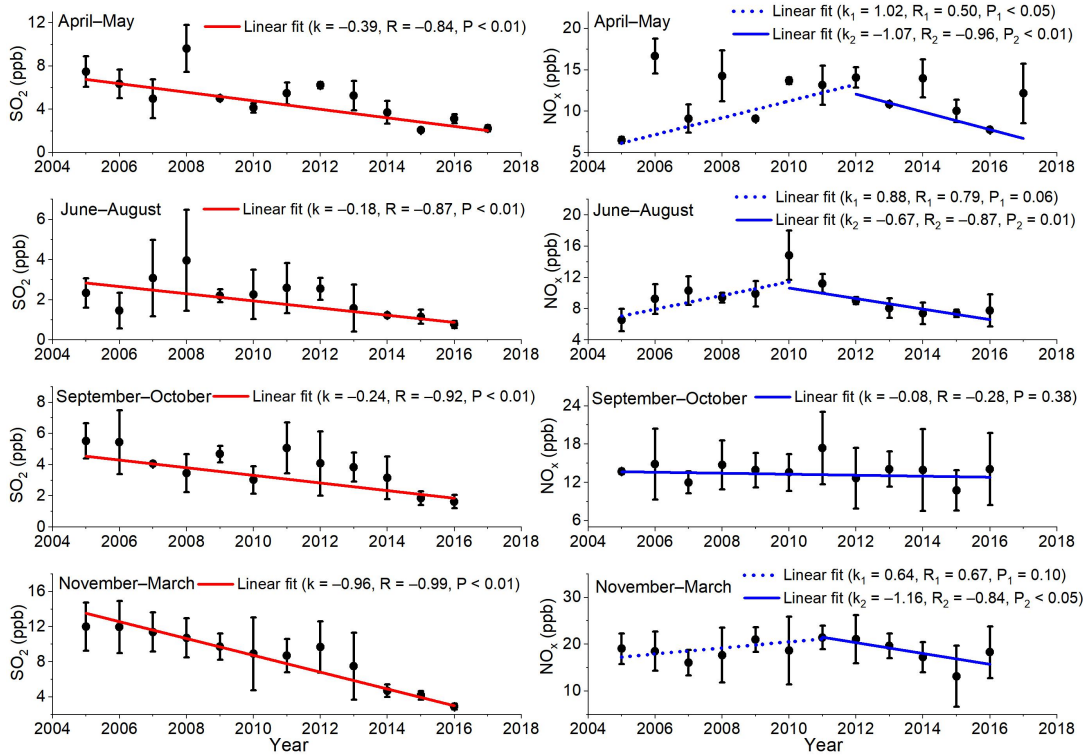


Figure 6. Long-term variations in monthly mean SO₂ and NO_x mixing ratios with $\pm 1\sigma$ in different periods at SDZ. Heating period (November–March next year), spring (April–May), summer (June–August), and autumn (September–October).

551

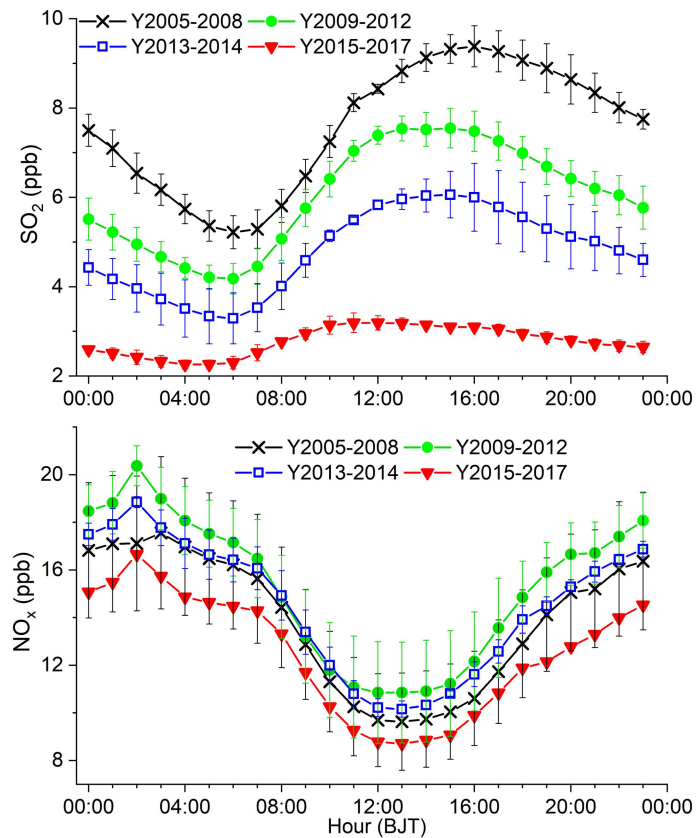
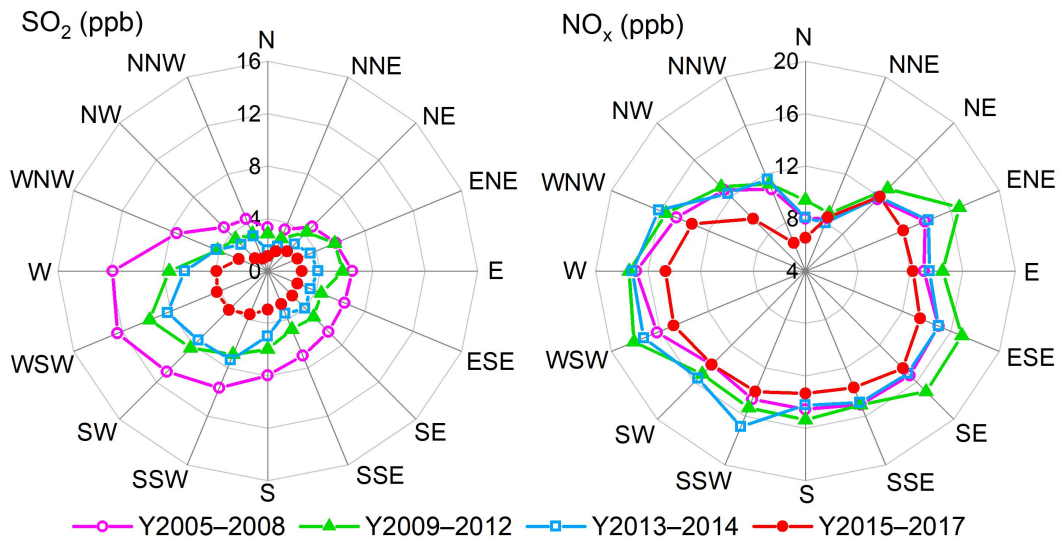
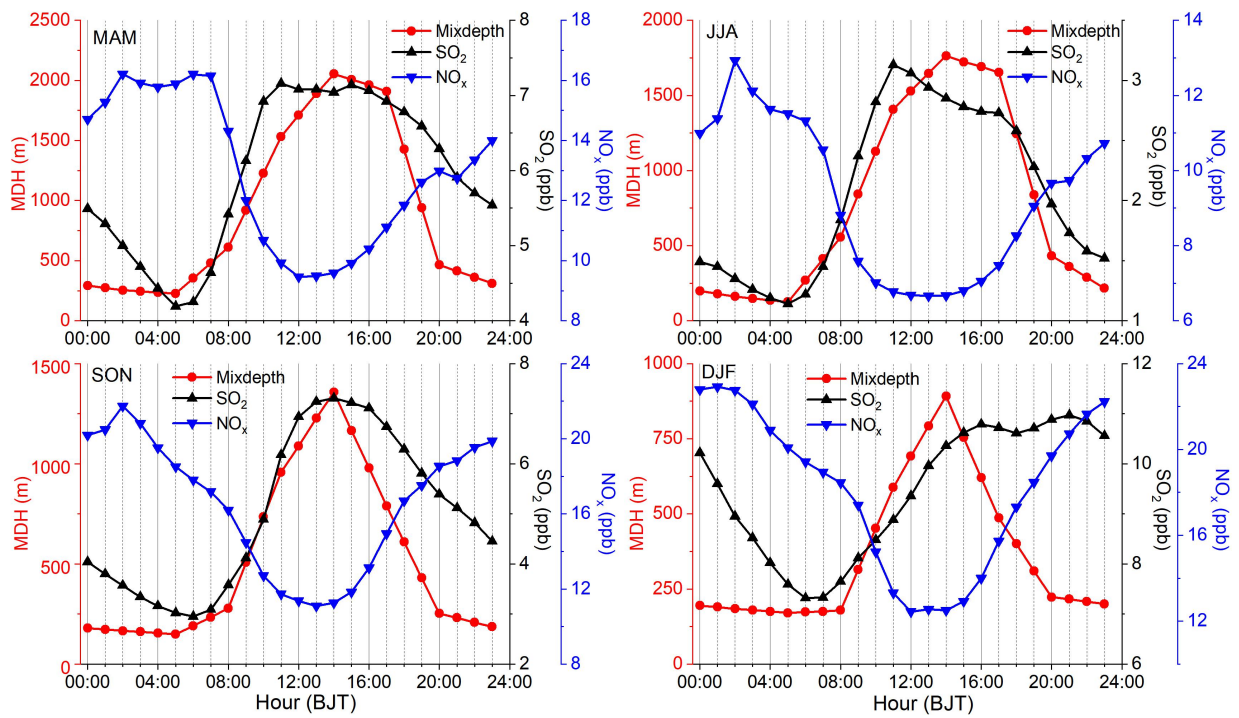


Figure 7. The average diurnal variations in SO₂ and NO_x mixing ratios in 4 different stages at SDZ.



552

Figure 8. Mixing ratios of SO_2 and NO_x during different stages as a function of wind direction at SDZ.



553

Figure 9. Diurnal variations in mixing depths in four seasons at SDZ.

Table 1. Statistics in the hourly mean of SO₂ and NO_x mixing ratios at SDZ.

	NO (ppb)	NO ₂ (ppb)	NO _x (ppb)	SO ₂ (ppb)
Mean	1.10	13.08	14.18	5.71
Standard deviation	2.58	10.89	12.36	8.44
Median	0.33	9.98	10.59	2.45
Maximum	83.34	124.41	147.58	100.34
Minimum	0.01	0.01	0.14	0.01
Count number	104923	104923	104923	105374

554

Table 2. NO_x and SO₂ levels in the atmospheric background stations in China.

Site	Time	NO _x (ppb)	SO ₂ (ppb)	References
SDZ (North China)	2005.1–2017.5	14.2 ± 12.4	5.7 ± 8.4	This study
Xinglong (North China)	2005.5–2015.1	–	7.5	(Bai et al., 2015)
Linan (Yangtze River Delta)	2005.8–2006.7	–	11.1 ± 10.6	(Qi et al., 2012)
	2006.1–2016.12	13.6 ± 1.2	7.0 ± 4.2	(Yin et al., 2022)
Wuyishan (East China)	2011.3–2012.2	2.70	1.48	(Su et al., 2013)
Dinghushan (South China)	2009.1–2010.12	13.6	6.5	(Chen, 2012)
Changbaishan (Northeast China)	2009.1–2010.12	4.7	2.1	(Chen, 2012)
Fukang (Northwest China)	2009.1–2010.12	8.3	2.2	(Chen, 2012)
Gonggashan (Southwest China)	2017.1–2017.12	0.90	0.19	(Cheng et al., 2019)
Jinsha (Central China)	2006.6–2007.7	5.6 ± 5.5	2.8 ± 5.5	(Lin et al., 2011b)

555

Table 3. Trends of the hourly mean of the three sectors with the highest SO₂ level, the hourly mean of the three sectors with the lowest SO₂ level and their difference.

	Highest SO ₂ values (ppb)	Lowest SO ₂ values (ppb)	Difference (ppb)
	W–WSW–SW–SSW sectors	NNW–N–NNE–NE sectors	
Y2005–2008	11.18	3.96	7.23
Y2009–2012	8.12	3.20	4.91
Y2013–2014	7.36	2.35	5.01
Y2015–2017	3.95	1.48	2.48

556